Phase Space of the Hydrogen Atom in a Circularly Polarized Microwave Field

Pol Navarro Pérez

July 1, 2025

Abstract

This study investigates the dynamics of the hydrogen atom subjected to circularly polarized microwave fields, with a focus on ionization processes and orbit classification. Starting from the simplest case ($K = 0$), we analyzed the behavior of unbounded regions and their role in leading to ionizing orbits as $K \neq 0$. Through numerical methods, we explored the influence of invariant manifolds and identified conditions that facilitate ionization.

Introduction: Dynamical Systems

Dynamical systems are mathematically modeled by equations such as:

$$x_{k+1} = f(x_k), \quad \text{for maps with } k \in \mathbb{Z}, \tag{1}$$

$$\frac{dx}{dt} = f(x), \quad \text{for vector fields with } t \in \mathbb{R}. \tag{2}$$

Sometimes, these equations cannot be solved analytically, requiring alternative methods to analyze the system's behavior. These methods provide a structured approach to explore the system and understand its dynamics.

Introduction: The CP Problem

In our reference paper [1], numerical methods are applied to a hydrogen atom interacting with a circularly polarized microwave field, known as the *CP problem*. The main goal is to study the electron's possible paths to escape or ionization, depending on its distance from the nucleus. The study of a dynamical system often starts by identifying the simplest solutions—equilibrium points—and exploring more complex structures such as:

- Stable and unstable manifolds,
- Homoclinic connections,
- Periodic orbits (PO),
- Invariant tori and bottlenecks near unstable POs.

These structures influence key transitions like ionization or escape.

Objectives of this Work

In this work, we closely follow the steps outlined in [1], sharing the same objectives:

- Explore methods to achieve similar conclusions through numerical techniques.
- Address computational challenges encountered and strategies employed.
- Critically assess the claims made and propose possible approaches.

The aim is not to replicate every graph presented but to provide insights into potential strategies and methodologies.

Hamiltonian of the CP Problem

The starting point is the Hamiltonian:

$$H = \frac{1}{2}(p_x^2 + p_y^2 + p_z^2) - \frac{1}{r} + F(x\cos(wt) + y\sin(wt)), \tag{3}$$

- (x, y, z): canonical coordinates.
- $r^2 = x^2 + y^2 + z^2$: distance to the nucleus.
- $F > 0$: field strength, w: angular frequency.

Simplifying the Hamiltonian and Equations of Motion

Transformations applied:

- Rotating frame with angular velocity w.
- Rescale time by $s = wt$.
- Symplectic change of variables:

$$(x, y) = a(\bar{x}, \bar{y}), \quad (p_x, p_y) = aw(\bar{p}_x, \bar{p}_y),$$

  where $a^3 w^2 = 1$.

Resulting simplified Hamiltonian:

$$H = \frac{1}{2}(p_x^2 + p_y^2) - (xp_y - yp_x) - \frac{1}{r} + Kx.$$

Equations of Motion:

$$x' = p_x + y, \quad y' = p_y - x,$$
$$p_x' = p_y - \frac{x}{r^3} - K, \quad p_y' = -p_x - \frac{y}{r^3}.$$

The equations satisfy the symmetry:

$$(t, x, y, p_x, p_y) \to (-t, x, -y, -p_x, p_y).$$

Equilibrium Points and Root Behavior

Finding the Equilibrium Points:

$$\begin{aligned} p_x + y = 0, \quad p_y - x = 0, \\ p_y - \frac{x}{r^3} - K = 0, \quad -p_x - \frac{y}{r^3} = 0. \end{aligned} \tag{4}$$

Reducing to:

$$f(x) = x^3 - Kx^2 - \mathrm{sign}(x).$$

- One root exists for $x > 0$ and one for $x < 0$ (Descartes' Rule of Signs).
- As $K \to 0$, roots approach $x = \pm 1$.

Behavior of Roots:

- For $x > 0$:

$$f(x) = x^3 - Kx^2 - 1, \quad x_2 > \max\left(1, \frac{2K}{3}\right).$$

- For $x < 0$:

$$f(x) = x^3 - Kx^2 + 1, \quad \max\left(-1, -\frac{1}{\sqrt{K}}\right) < x_1 < 0.$$

Equilibrium Points: Numerical Results

K		L_1	L_2
0.0015749	x	-0.99947531	1.00052524
	h	-1.50157449	-1.49842469
	λ_i	$-0.0687, 0.0687$	$-0.0687, 0.0687$
0.1	x	-0.9761	1.0345
	h	-1.4212	-1.3983
	λ_i	$-0.5304, 0.5304$	$-0.5304, 0.5304$

Table: Equilibrium points, energies, and eigenvalues for $K = 0.0015749$ and $K = 0.1$.

Stability of Equilibrium Points

To analyze stability, we compute the Jacobian matrix at equilibrium points:

$$Df(x, y, p_x, p_y) = \begin{pmatrix} 0 & 1 & 1 & 0 \\ -1 & 0 & 0 & 1 \\ \frac{2x^2-y^2}{r^5} & \frac{3xy}{r^5} & 0 & 1 \\ \frac{3xy}{r^5} & \frac{2y^2-x^2}{r^5} & -1 & 0 \end{pmatrix},$$

where $r = \sqrt{x^2 + y^2}$. Substituting equilibrium points $(x_i, 0, 0, x_i)$, the Jacobian simplifies to:

$$Df(x_i, 0, 0, x_i) = \begin{pmatrix} 0 & 1 & 1 & 0 \\ -1 & 0 & 0 & 1 \\ \frac{2}{|x_i|^3} & 0 & 0 & 1 \\ 0 & -\frac{1}{|x_i|^3} & -1 & 0 \end{pmatrix}.$$

Definitions and Stability Theorem

Definitions:

- An equilibrium point p is **hyperbolic** if all eigenvalues of $A := Df(p)$ have real parts different from 0.
- An equilibrium point p is **elliptic** if all eigenvalues of $A := Df(p)$ have purely imaginary parts, with a diagonal Jordan matrix.

Stability Theorem:

Theorem (Stability of Equilibrium Points)

For a dynamical system $\dot{x} = f(x)$ with equilibrium point p:

1. *If all eigenvalues of $Df(p)$ have real parts < 0, then p is* ***asymptotically stable****.*
2. *If any eigenvalue has a real part > 0, then p is* ***unstable****.*

Stability Analysis of x_1 and x_2

Stability of x_1: For $x_1 < 0$, eigenvalues simplify to:

$$\pm\sqrt{\frac{1 + 2x_1^3 \pm \sqrt{8x_1^3 + 9}}{2|x_1|^3}}.$$

- Two real eigenvalues and two purely imaginary eigenvalues.
- x_1 is a *center* $\times$ *saddle* and unstable.

Stability of x_2: For $x_2 > 0$, eigenvalues simplify to:

$$\pm\sqrt{\frac{1 - 2x_2^3 \pm \sqrt{9 - 8x_2^3}}{2x_2^3}}.$$

- For $K \leq 0.1156$, all eigenvalues are purely imaginary: x_2 is a *center* $\times$ *center*.
- For $K > 0.1156$, eigenvalues become complex: x_2 transitions to a *complex saddle*.

Hill's Regions

Hill's regions reveal the spatial configurations where motion is **energetically allowed** or **forbidden**, determined by the condition:

$$h + \left(\frac{y^2}{2} + \frac{x^2}{2} + \frac{1}{r} - Kx \right) \geq 0.$$

These regions depend on the parameters h (energy) and K (field strength), providing insights into the system's constraints and behavior.

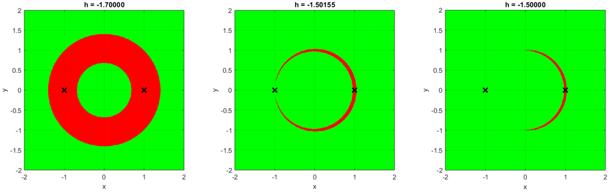

Figure: Hill's regions for $K = 0.0015749$: $h = -1.7$ (left), $h = -1.50155$ (center), and $h = -1.5$ (right). Green: allowed regions, red: forbidden. Equilibrium points are marked with crosses.

Hill's Regions for $K = 0.1$

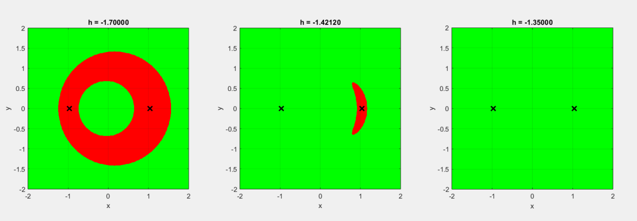

Figure: Hill's regions for $K = 0.1$ with energies above, below, and between L_1 and L_2.

Introduction to Homoclinic Connections

We analyze the dynamics around equilibrium points by introducing the concepts of **stable** and **unstable manifolds**, fundamental for understanding orbit structures.

Theorem (Stable and Unstable Manifolds)

Let $\phi(t, x)$ represent the flow of a dynamical system. The local stable and unstable manifolds of an equilibrium point p are defined as:

- **Local Stable Manifold:**

$$W^s_{loc}(\epsilon) = \{x \in \mathbb{R}^n \mid \|\phi(t, x) - p\| < \epsilon,\ t \geq 0\}.$$

Points converge to p as $t \to +\infty$.

- **Local Unstable Manifold:**

$$W^u_{loc}(\epsilon) = \{x \in \mathbb{R}^n \mid \|\phi(t, x) - p\| < \epsilon,\ t \leq 0\}.$$

Points approach p as $t \to -\infty$.

Homoclinic and Heteroclinic Orbits

Definition: Homoclinic Orbit

$$\phi(t,x) \in W^s(p) \cap W^u(p), \quad \lim_{t\to\pm\infty} \phi(t,x) = p.$$

Definition: Heteroclinic Orbit

$$\phi(t,x) \in W^u(p) \cap W^s(q), \quad \begin{array}{l} \lim_{t\to+\infty} \phi(t,x) = p, \\ \lim_{t\to-\infty} \phi(t,x) = q. \end{array}$$

These definitions are fundamental for understanding the connections between invariant sets in phase space.

Manifolds of the CP Problem

We analyze the **local stable and unstable manifolds** of the saddle-type equilibrium point L_1.

- Example parameters: $K = 0.1$, $h = -1.7$.
- Equilibrium points:

$$x_1 = -0.967753, \quad h_1 = -1.5983, \quad x_2 = 1.034469, \quad h_2 = -1.3982.$$

- For x_1, eigenvalues are:

$$\lambda_1 = -0.530370, \quad \lambda_2 = 0.530370.$$

  - **Stable manifold (W^s)**: Aligned with the eigenvector of λ_1 (negative real part).
  - **Unstable manifold (W^u)**: Aligned with the eigenvector of λ_2 (positive real part).
- L_1 is classified as a **saddle point**, where:
  - Trajectories **converge** along W^s.
  - Trajectories **diverge** along W^u.

Computing and Visualizing the Manifolds

Initial Points:

$$x_{\text{stable},\pm} = x_1 \pm s \cdot v_{\text{stable}}, \quad x_{\text{unstable},\pm} = x_1 \pm s \cdot v_{\text{unstable}}, \quad s = 10^{-6}.$$

Numerical Integration:

- **Stable manifold (W^s)**: Integrated **backward** in time (converges to L_1).
- **Unstable manifold (W^u)**: Integrated **forward** in time (diverges from L_1).

Visualization ($K = 0.1$, $h = -1.7$):

- Intersection of W^u_+ and W^s_-: **outer connections**.
- Intersection of other branches: **inner connections**.

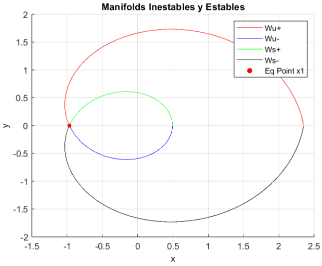

Figure: Manifold branches around x_1.

Homoclinic Connections and Manifold Behavior

Manifold Behavior:

- The unstable branch W^u_- for $K = 0.1$ and $h = -1.7$ remains **bounded** within the inner region.
- It does not form a **periodic orbit**.

Homoclinic Connections:

- Occur when W^s and W^u intersect.
- **Symmetry:**

$$(t, x, y, p_x, p_y) \to (-t, x, -y, -p_x, p_y).$$

- A perpendicular intersection ($x' = 0$) at $y = 0$ implies **symmetric homoclinic orbits**.
- These trajectories depart along W^u and return along W^s, forming a closed path in phase space.

Relation to Lyapunov Periodic Orbits (LPOs):

- By computing x' at crossing points of W^u with $y = 0$, we analyze conditions for **homoclinic orbits** and **periodic orbits**.

Analysis of x' at Crossing Points

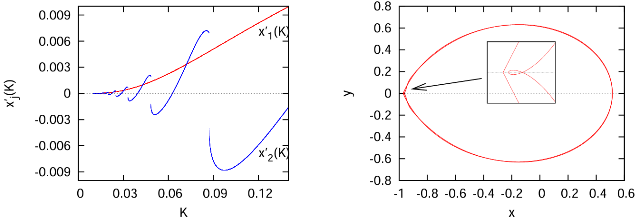

Figure: x_j' (derivative at j-th crossing) for various K values and $y = 0$. From [1]

- Homoclinic connections are absent for $j = 1$ crossings around L_1.
- For $j = 2$, infinite symmetric homoclinic orbits exist ($x_2'(K) = 0$).
- As K decreases, x' approaches zero, increasing the likelihood of symmetric homoclinic orbits.

Remark: Discontinuities in x'

Discontinuities in x' arise from loops in the orbits intersecting the Poincaré section at different points.

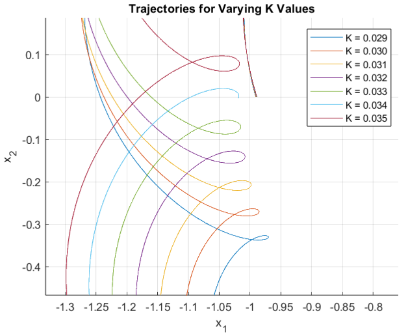

Figure: Loops from the unstable negative branch for various K values.

Example of a Homoclinic Connection

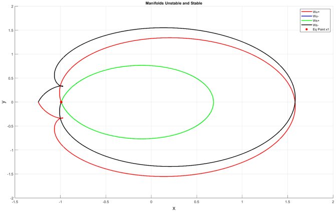

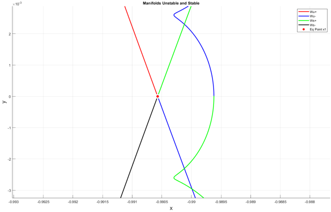

Figure: Negative branch of W^u for $K = 0.02855986$ up to the second crossing at $y = 0$.

Transit and Non-Transit Orbits

- **Transit Orbits:** Trajectories crossing the bottleneck region (defined by zero-velocity curves), transitioning between inner and outer regions.
- **Non-Transit Orbits:** Trajectories confined to their respective regions, bouncing back from the bottleneck.
- For K small and $h_1 < h < h_2$:
  - Specific orbits repeatedly transition between inner and outer regions.
  - Invariant tori act as barriers in phase space, preventing ionization.

Introduction to Periodic Orbits

- Periodic orbits (POs) are trajectories where the system returns to its initial state after a fixed period.
- Classification of POs provides insights into stability, bifurcations, and the dynamics of the Circular Planar (CP) problem.

Key Definitions:

Definition

A trajectory $\phi(t, x)$ is T-**periodic** if:

1. $\phi(T, x) = x$,
2. $\phi(t, x) \neq x$ for $0 < t < T$.

Definition

A periodic orbit is classified as:

- **Direct:** If its projection in the (x, y)-plane moves counterclockwise.
- **Retrograde:** If it moves clockwise.

Stability of Fixed Points

Theorem (Stability of Fixed Points)

Consider the discrete dynamical system:

$$x_{n+1} = f(x_n),$$

with equilibrium point p. Then:

1. *If all eigenvalues of $A := Df(p)$ have modulus < 1, then p is* **asymptotically stable**.
2. *If any eigenvalue of A has modulus > 1, then p is* **unstable**.

Floquet Multipliers:

- The eigenvalues of the monodromy matrix M determine the stability of a periodic orbit.
- A PO is **linearly stable** if all Floquet multipliers lie on or within the unit circle, except a simple 1 due to time invariance.

Numerical Computation: Poincaré Section

- A Poincaré section is defined as $x' = 0$ and $y' < 0$.
- Initial conditions are iteratively refined using a bisection method to satisfy $x' = 0$, ensuring symmetry.
- Figure 7 shows symmetric periodic orbits for $K = 0.0015749$ and $h = -1.7$.

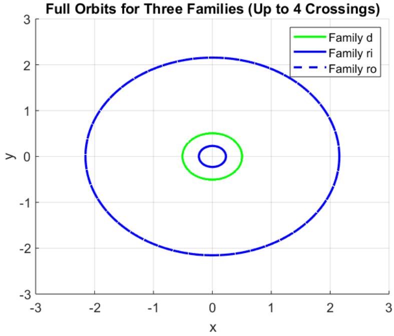

Figure: Periodic orbits for $K = 0.0015749$ and $h = -1.7$.

Periodic Orbits and Families

- For $K = 0$, three PO families exist:
  - d: Direct periodic orbits in the bounded Hill region.
  - ri: Retrograde orbits in the bounded region.
  - ro: Retrograde orbits in the unbounded region.
- For $K > 0$ (small), these families persist with minor changes:
  - Family d: Exists for $h < h_1$; period tends to infinity as $h \to h_1$.
  - Family ri: Exists for all h; period varies between $[0, 2\pi]$.
  - Family ro: Alternating stability, bifurcates into new families.

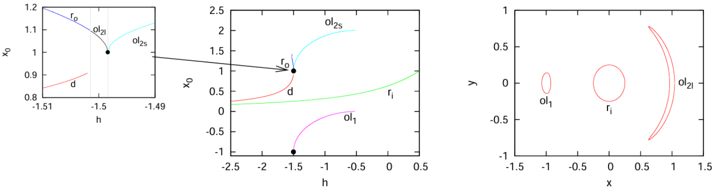

Figure: Characteristic curves and periodic orbits for $K = 0.0015749$. From [1]

Lyapunov Orbits and Equilibrium Points

Lyapunov Orbits:

- Based on **Lyapunov's Theorem**, families of Lyapunov periodic orbits (LPOs) emerge near equilibrium points.
- Example for $K = 0.0015749$:
  - $x_1 = -0.99947531$, $h_1 = -1.50157449$ (**Saddle × Center**).
  - $x_2 = 1.00052524$, $h_2 = -1.49842469$ (**Center × Center**).

Analysis of Equilibrium Points:

Energy	**Eigenvalues**
$h_1 = -1.50157449$	$\pm 0.0687, \pm 1.0016i$

Table: $x_1 = -0.99947531$: Saddle × Center.

Energy	**Eigenvalues**
$h_2 = -1.49842469$	$\pm 0.0688i, \pm 0.9984i$

Table: $x_2 = 1.00052524$: Center × Center.

Lyapunov Orbits: Examples

- Families of LPO:
  - ol_1: Unstable, $T = 2\pi/1.00157 \approx 6.27$.
  - ol_{2l}: Linearly stable, $T = 2\pi/0.9984 \approx 6.29$.
  - ol_{2s}: Short period, linearly stable.

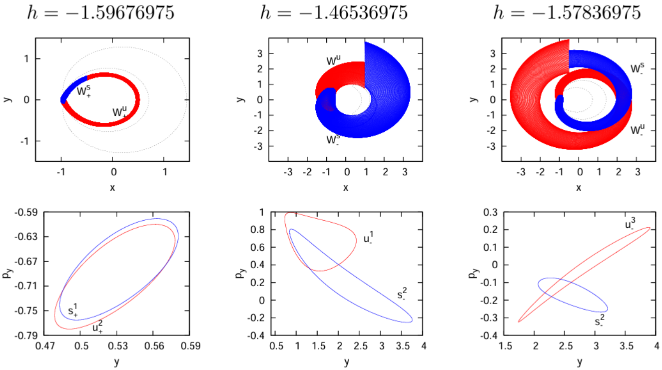

Figure: LPOs in configuration space for $K = 0.1$. From [1]

Transit and Non-Transit Orbits

- **Transit Orbits:** Cross bottleneck region, transition between inner and outer regions.
- **Non-Transit Orbits:** Confined to initial region.

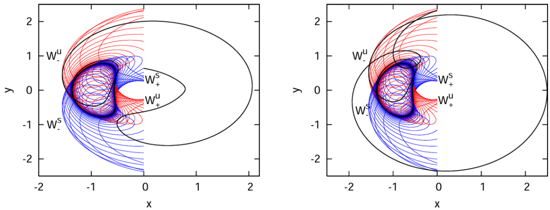

Figure: Comparison of transit (a) and non-transit (b) orbits. From [1]

Ionization Dynamics: $K = 0$

Regular Dynamics:

- **Integrable case:** Rotating two-body problem.
- Types of orbits:
  - Rotating ellipses (bounded).
  - Parabolas (boundary between bounded and unbounded).
  - Hyperbolas (unbounded).
- Dynamics:
  - Invariant curves in Poincaré Surface of Section (PSP).
  - Smooth transition between orbit types.

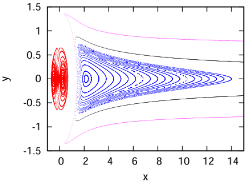

Figure: PSP for $K = 0$: Regular orbits around bounded/unbounded regions. From [1]

Ionization Dynamics: $K > 0$

Chaotic Dynamics:

- **Non-integrable case:** Chaos emerges due to resonance overlap.
- Key phenomena:
  - Destruction of invariant curves (**KAM Theorem**).
  - Emergence of chaotic layers and erratic trajectories.
  - Long escape times and slow ionization.
- Example: $K = 0.0015749, h = -1.7$.

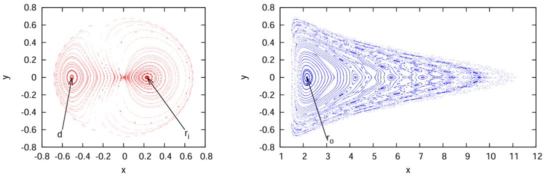

Figure: PSP for $K = 0.0015749$ and $h = -1.7$: Chaotic layers and resonances. From [1]

Dynamics for $h < h_1$

- Configuration space divided into bounded and unbounded regions by Hill's region boundaries.
- At $h = -1.7$:
  - Bounded region: resembles the rotating two-body problem with stable periodic orbits surrounded by invariant curves.
  - Unbounded region: dynamics become irregular as $K > 0$, with chaotic layers, periodic orbits, and regions of stochasticity.
  - Farther from the origin: invariant curves break into chains of islands and hyperbolic orbits.
- Erratic trajectories transition between islands, showing structured stochasticity influenced by hyperbolic orbits and heteroclinic connections.

Quasi-Periodic Orbits

- Invariant curves in the Poincaré section correspond to quasi-periodic orbits.
- These orbits densely fill a torus in phase space without forming closed trajectories.

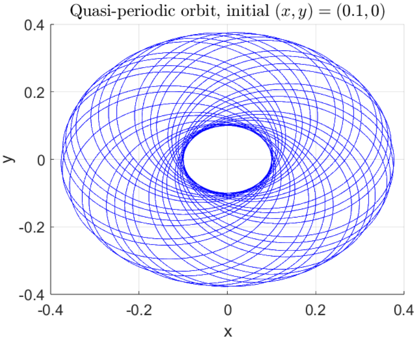

Figure: Quasi-periodic orbit for initial conditions from an invariant curve.

Dynamics for $h \in (h_1, h_2)$

- Example: $h = -1.5$, ZVC forms a bounded, right-moon-shaped region intersecting the x-axis at two points.
- For $h = h_1$: The equilibrium point L_1 emerges, and orbits collapse into its stable and unstable manifolds.
- For $h > h_1$:
  - Neck connects inner and outer regions, removing motion barriers near the origin.
  - Periodic orbits of families $ol1$, ri, and $ol2l$ observed.

PSP for $K = 0.0015749$ and $h = -1.5$

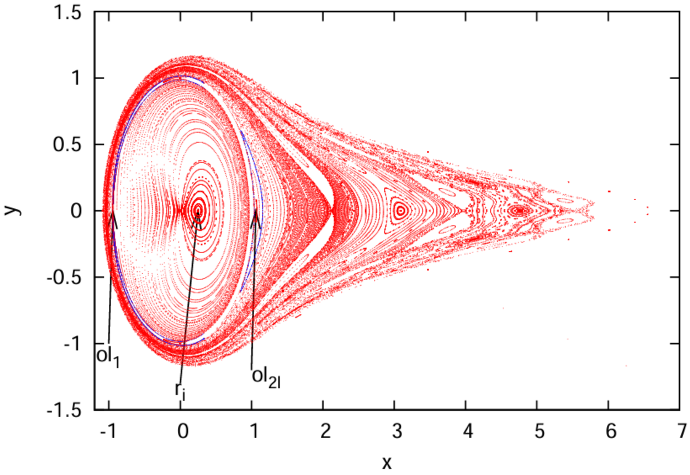

Figure: PSP showing the orbits of the main families ($ol1, ri, ol2l$) and the moon-shaped forbidden region. From [1].

Dynamics for $h > h_2$

- No zero-velocity curve (ZVC) exists at these energy levels.
- System features:
  - Stable retrograde orbit (ri).
  - Short-period Lyapunov periodic orbit (LPO) around L_2.
  - Hyperbolic LPO around L_1, with stable (W^s) and unstable (W^u) invariant manifolds.
- A last invariant curve surrounds the origin, confining $o/1$ family manifolds.
- Outside this curve: chaotic behavior dominates, with erratic and ionizing orbits appearing.

Phase Space Plot ($K = 0.0015749, h = -0.557$)

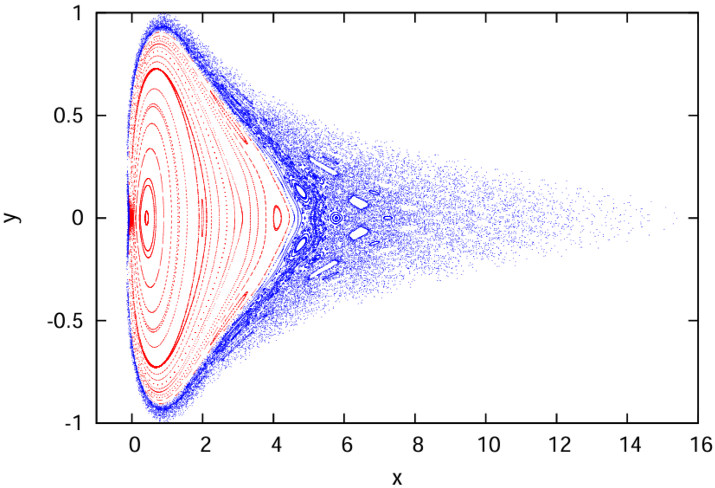

Figure: PSP for $K = 0.0015749$ and $h = -0.557$, showing points (x, y) evaluated at $x' = 0$, $y' < 0$. From [1].

Radial Distances Comparison around L_1

By experimenting with the code, we can observe these differences directly. The following image illustrates the radial distances for the nucleus, comparing cases with $h > h_2$ for both a small and a large K, following the unstable negative branch of the manifold around L_1.

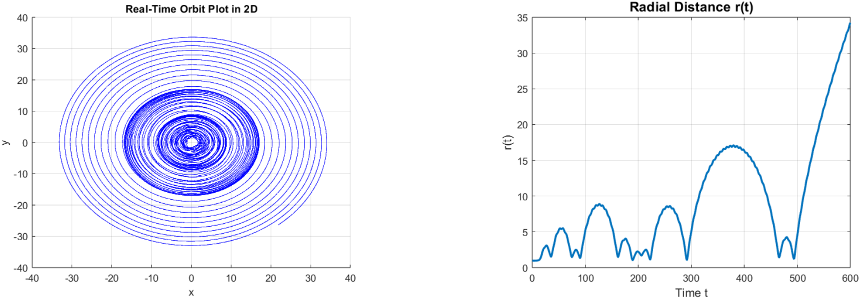

Figure: W^u_- orbit and radial distance around L_1 for a high value $K = 0.1$ and a fixed high value $h = -1$.

Radial Distance Analysis (1/2)

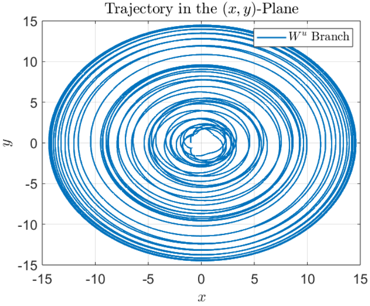

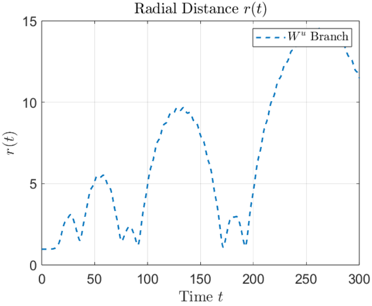

Radial Distance Analysis (2/2)

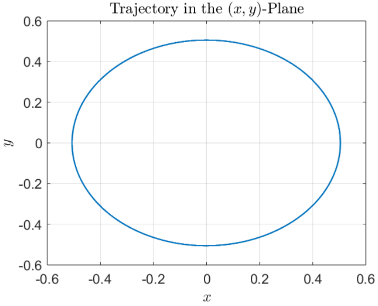

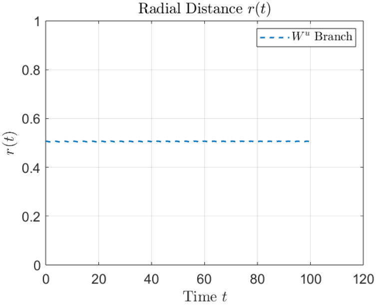

Comments on Escape Rates

In this section, we analyze the **phase space dynamics** to provide quantitative predictions for escape rates. The system exhibits different types of trajectories:

- **Fast Ionization (FI):**
  - Trajectories **spiral outward** without revisiting the nucleus.
  - Nearly **radial in rotating coordinates**, resembling **hyperbolas in inertial coordinates**.
  - Escape occurs **rapidly**, with **minimal oscillations** in $r(t)$ over time.
- **Slow Ionization (SI):**
  - Erratic behavior with **successive approaches** to and **recedes from** the nucleus.
  - Alternates between **maxima and minima** of $r(t)$, with no clear trend.
  - Dynamics dominated by **interactions of invariant manifolds** and the chaotic region.

Ionization Pathways

Criterion for Hyperbolic Behavior (Fast Ionization - FI):

- The osculating sidereal energy $E_s(t)$ is used:

$$E_s = \frac{1}{2}(X'^2 + Y'^2) - \frac{1}{\sqrt{X^2 + Y^2}},$$

  where X, Y are positions and X', Y' are velocities in the non-rotating frame.
- An orbit is **hyperbolic** if $E_s(t) > \delta > 0$ for a small threshold δ.
- Orbits with this condition exhibit **fast escape** characterized by continuous growth in distance.

Classification of Other Orbits (EBE):

- Parameters T (observation time) and D (critical distance):
  - Typical values: $T = 5 \times 10^4$, $T = 10^5$, and $D = 100$.
- Effective Bounded Erratic (EBE) orbits:
  - Confined within D and satisfy $E_s(t) \leq 0$ for $t \leq T$.
  - Periodic orbits always meet these criteria.
  - Other trajectories may transition to FI as T or D increase.

Osculating Sidereal Energy: Definition and Region

Initial Conditions:

- Region: $(x_0, \theta) \in [x_m, \infty) \times [0, 2\pi)$, where $\theta = 0$ and $\theta = 2\pi$ are identified.
- Focuses on the right-hand side of the zero-velocity curve ($x_0 > x_c$), avoiding initial conditions near the nucleus.

Two-Body Problem Approximation:

$$E_s^0 = \frac{v^2}{2} + \frac{x_0^2}{2} + x_0 v \sin\theta - \frac{1}{x_0},$$

where v is determined from the constraints of the problem.

Erratic Region R:

- Defined by $E_s^0 < 0$, identifying erratic or escaping orbits.
- Boundary equation:

$$\sin\theta = \frac{-h - x_0^2 + Kx_0}{vx_0}.$$

Properties of the Erratic Region R

Behavior of R:

- For $h < -\frac{1}{2K}$:
  - R is empty since $f(x_0) = \frac{-h - x_0^2 + Kx_0}{vx_0} < -1$.
- For $h > -\frac{1}{2K}$:
  - $f(x_0)^2 = 1$ has two solutions:

$$\tau_{1,2} = \frac{1 + Kh \pm \sqrt{1 + 2Kh}}{K^2}.$$

  - R is bounded within $x_0 \in (\tau_1, \tau_2)$.

Shape of R:

- As x_0 increases, R takes a **"spear-like"** shape symmetric around $\theta = 3\pi/2$.
- For small K, the extent of R can grow significantly ($\sim 2/K^2$).

Visualization of Regions Based on E_s^0

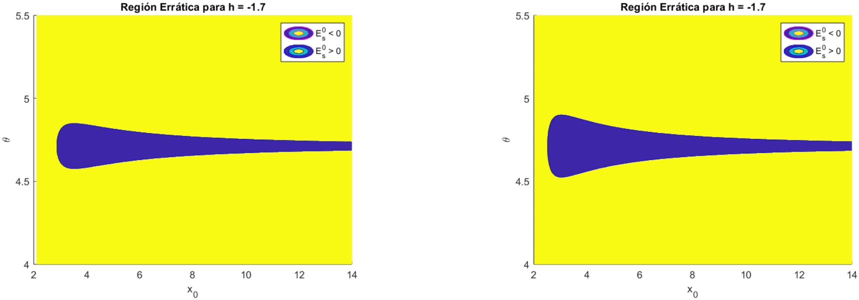

Figure: Regions depending on E_s value for $h = -1.7$ and a) $K = 0.0015749$ b) $K = 0.1$.

Dynamics of FI and EBE Orbits

- For small values of K:
  - Orbits that do not enter the vicinity U of the origin typically exhibit **Fast Ionizing (FI) behavior**.
  - The erratic region (R) has a bottleneck shape and becomes thinner as x_0 increases.
- There is a maximum value $x_{0,M} \approx \frac{2}{K^2}$, beyond which all initial conditions lead to FI orbits.
- The system exhibits a coexistence of:
  - Regular (periodic and quasiperiodic) orbits.
  - Stochastic regions with EBE orbits.

FI and EBE Orbits Visualization

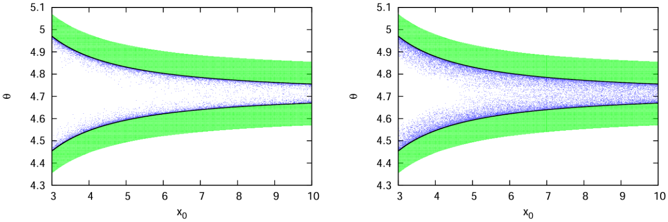

Figure: Illustration of Fast Ionizing (FI) and Erratic Bounded Escape (EBE) orbits for small K. The bottleneck-shaped region R becomes thinner as x_0 increases, highlighting the transition between behaviors. From [1].

Conclusions

- Hydrogen atom dynamics under circularly polarized microwave fields were studied.
- Key findings:
  - $K = 0$: Unbounded regions lead to ionizing orbits.
  - $K > 0$: Manifolds crucially influence ionization.
  - Rich dynamics in unconfined regions, leading to EBE or FI behavior.
- Numerical challenges:
  - Pseudo-arc method faced convergence issues for G.
  - Poincaré Section Plot generation suboptimal in implementation.
  - Certain results taken from the reference study for clarity.
- Emphasis on methodologies to compute graphs and analyze results.

References I

Barrabés, E., Ollé, M., Borondo, F., Farrelly, D., & Mondelo, J. M. (2012). *Phase space structure of the hydrogen atom in a circularly polarized microwave field*. Physica D: Nonlinear Phenomena, 241(4), 333-349.

Astakhov, S. A., Burbanks, A. D., Wiggins, S., & Farrelly, D. (2003). *Chaos-assisted capture of irregular moons*. Nature, 423(6937), 264–267.

Sugon Jr, Q., Bennett, C. D. G., & McNamara, D. J. (2024). *Hydrogen atom as a nonlinear oscillator under circularly polarized light: epicyclical electron orbits*. arXiv preprint arXiv:2410.00056.

Fejoz, J., & Guardia, M. (2023). *A remark on the onset of resonance overlap*. Regular and Chaotic Dynamics, 28(4), 578-584.